Swiss J Geosci (2013) 106:91–107
DOI 10.1007/s00015-013-0122-z

Growth-strata geometry in fault-propagation folds: a case study from the Gafsa basin, southern Tunisian Atlas

Riadh Ahmadi · Eric Mercier · Jamel Ouali

Received: 19 July 2012 / Accepted: 25 February 2013 / Published online: 24 May 2013

Abstract The structural and sedimentological study of fault-propagation folds in Southern Tunisia highlights a special geometry of the growth strata (strata deposited simultaneously with the formation or growth of a fold). This distinct geometry is visible in the uppermost growth-strata beds and consists of one flank with unconformity as opposed to the other flank with perfect conformity. This geometry can be explained by the mechanism of fault-propagation folding, with asymmetrical flank dips and hinge migration kinematics. This kinematics was originally predicted by the fault-propagation fold model, which facilitates the study of this special geometry in a narrow domain of sedimentation-to-shortening ratios. A plot projection provides a generalisation of the results of all types of fault-propagation folds by revealing the expected geometry of the growth strata. This study constitutes one of the most complete examples of kinematic model validation on a field scale.

Keywords Tunisian Atlas · Fold mechanisms · Fault-related folding · Growth-strata · Fold hinge migration

Editorial Handling: A. G. Milnes.

Electronic supplementary material The online version of this article (doi:10.1007/s00015-013-0122-z) contains supplementary material, which is available to authorized users.

R. Ahmadi (✉) · J. Ouali
Laboratoire LR3E, Ecole Nationale d'Ingénieur de Sfax, BP W 3038 Sfax, Tunisie
e-mail: riadhahmadi@yahoo.fr

E. Mercier
Planétologie et Géodynamique (UMR 6112), Université de Nantes, BP 92208, 44322 Nantes Cedex 3, France

1 Introduction

Several methods and techniques have been developed that are based on growth-strata geometry (the geometry of strata deposited simultaneously with the formation or growth of a fold) as they relate to fold kinematics (Zoetmeijer 1993; Shaw and Suppe 1994; Poblet and Hardy 1995; Hardy and Poblet 1994; Wickham 1995; Zapata and Allmendinger 1996; Hardy 1997; Muller and Suppe 1997; Storti and Poblet 1997; Suppe et al. 1997; Salvini et al. 2001; Salvini and Storti 2002; Bernal and Hardy 2002; Grando and McClay 2004; Tavani et al. 2007). These geometric models describe the projected geometry of the growth strata during folding. The particular geometries observed in growth strata are linked to hinge kinematics. All models are in agreement with the specific growth-strata geometry for each of the fold model kinematics (e.g. Fig. 1). Consequently, growth-strata geometry can be an efficient method for the study of fold kinematics, which is essential for modelling (Hardy and Poblet 1994; Ahmadi et al. 2006; Mercier et al. 2007; Livio et al. 2009). The current discussion concerns the hinge behaviour of fault-related folds and detachment folds mainly within the growth strata. The main question is whether the hinges are fixed with respect to the material or whether the hinges migrate during the growth of the fold (Mercier et al. 2007). Because the demonstration of growth-strata geometry and fold kinematics with field or geophysical data is particularly challenging, the fixed-hinge theory appears to be the dominant theory.

Other important parameters, such as sedimentation rate and uplift rate, also control the final growth-strata geometry (Fig. 1). The uplift rate was originally applied by several authors to determine the vertical uplift of the anticline crest. The uplift rate can be expressed with the same units

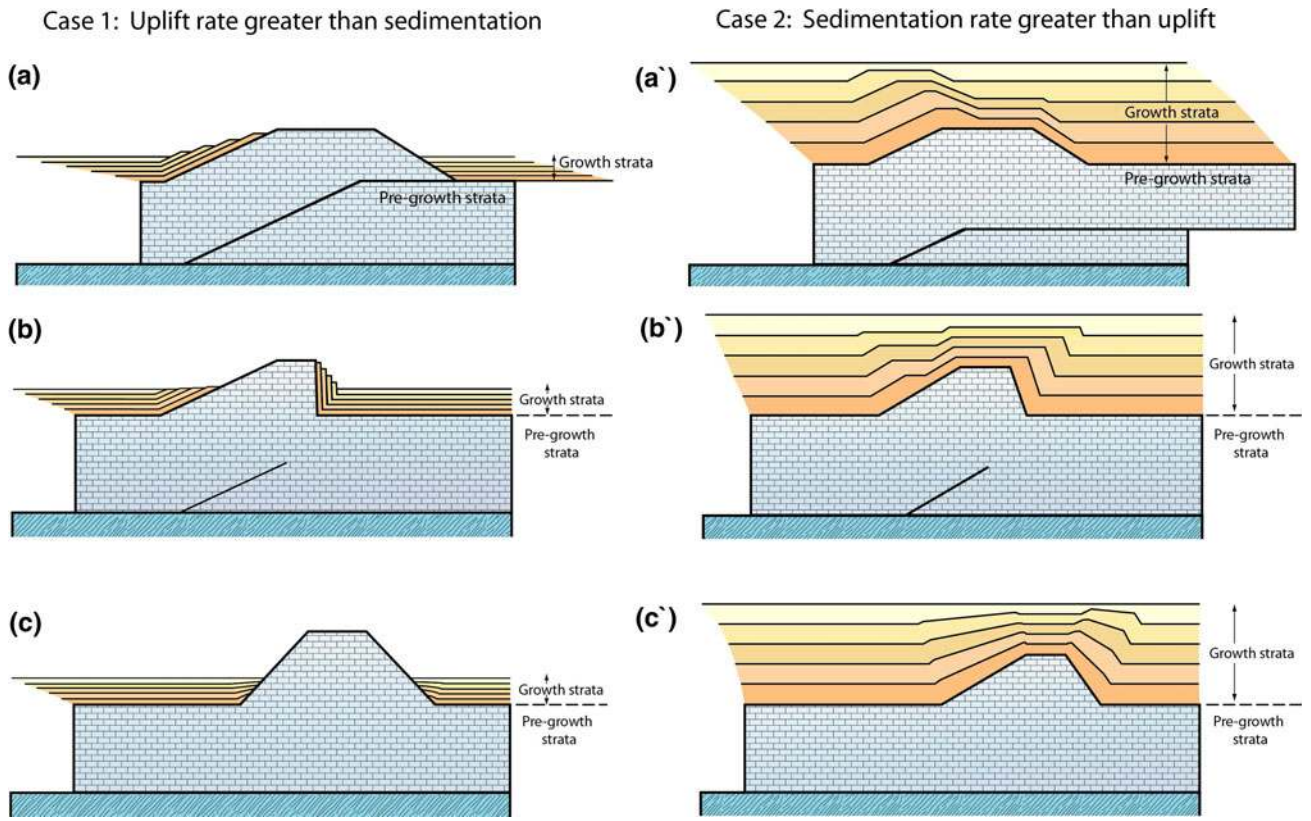

Fig. 1 Examples of fold models and their expected growth-strata geometry. Case 1 describes geometries when the uplift rate is greater than the sedimentary rate (which causes all fold types to emerge at the surface), case 2 is obtained when the sedimentation rate is greater than tectonic uplift, and the fold does not emerge from the basin (the case treated here using modelling software developed from the work of Rafini and Mercier 2002). Models **a** and **a′** fault-bend fold, models **b** and **b′** fault-propagation fold and models **c** and **c′** detachment fold

as for the sedimentation rate (e.g. m/Ma). This uplift rate is dependent on horizontal shortening, which is the deformation rate. However, for hinge migration folds, the uplift rate is also dependent on limb dips that consequently caused them to develop into asymmetric folds. In the present paper, the deformation rate will be used to independently compute the local uplift value for each flank.

The ratio of the sedimentation rate to the uplift rate (R) controls the morphology of the fold. With a high sedimentation-to-uplift ratio (R >1), the anticline structure remains immersed in the basin beneath the growth strata (Fig. 2). This is particularly true for offshore anticlines with low amplitude, as seen on many seismic profiles. Unless the seismic data are of very good quality (e.g. 3D high resolution), it is difficult to identify essential features that characterise the probable kinematics. These difficulties are due to the following reasons:

1. In basin examples with high sedimentation-to-uplift ratios, the specific markers that could indicate the kinematics are smaller, which makes observation more difficult due to the low deformation amplitude (e.g. Suppe et al. 1992; Shaw and Suppe 1994). Practically only high definition 3D seismic data is able to highlight such markers (Livio et al. 2009).
2. Few basin examples exist under the conditions described above, and there is a lack of interest in hydrocarbon exploration. For this reason, only a few authors have revealed partially studied examples (e.g. Tavani et al. 2007), and none have described a complete case study of fold models and their entire growth-strata complex.

Low sedimentation-to-uplift ratios (R <1) typically cause the anticline structure to emerge from the basin (Fig. 2). This case is true for most of the continental folds found in nature. The sedimentary series of growth strata are created by erosion processes and consist mainly of clastic sediments. In such cases, the growth strata are subject to deep erosion because of the softness and low cohesion of material that is associated with nearby active anticline structures.

Only a limited number of natural case studies have succeeded in establishing a distinct relationship between growth-strata geometry and fold kinematics in continental domains. The work of Rafini and Mercier (2002) demonstrated that hinge migration had taken place on the Sant

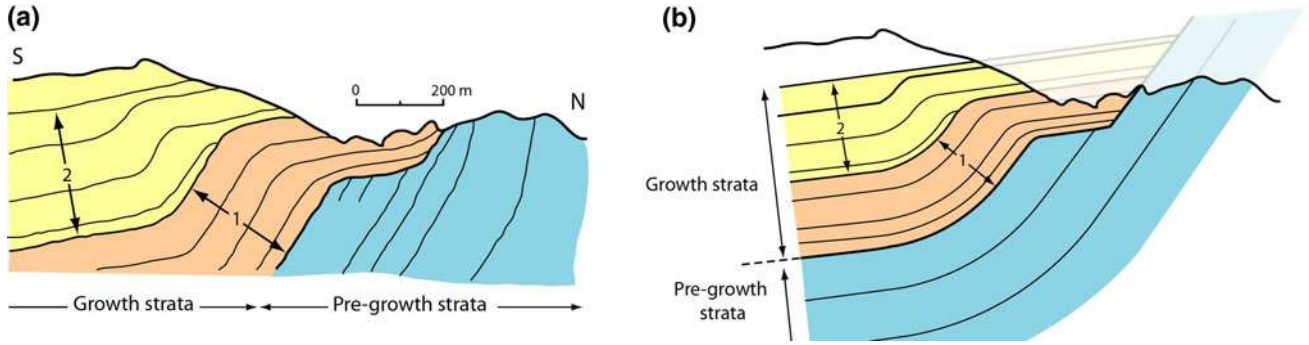

Fig. 2 Growth-strata geometry in Sant Lorenç region, northern Spain. In this example, the numbers *1* and *2* correspond to two sequences of growth strata separated by a hinge migration tectonic event. **a** Cross section adapted after Ford et al. (1997). **b** Model simulation adapted from Rafini and Mercier (2002)

Llorenç de Morunys anticline flank (northern Spain) by using growth-strata forward modelling. They achieved successful results (Fig. 2) without establishing a model of the original fold. This interesting cross section was initially described by Riba (1976) then a detailed geometrical characterisation was performed by Ford et al. (1997). Based on the latter, Suppe et al. (1997) concluded that the syncline had formed by hinge migration, and finally Rafini and Mercier (2002) succeeded in building a numerical model for this cross-section.

Ahmadi et al. (2006) studied growth strata related to the Alima anticline in southern Tunisia. In that case, a fault-propagation model for the fold was proposed, based on geometric and morphological arguments. The growth strata were deeply eroded with the exception of a newly formed thin pediment that exhibited a shoulder shape deformation, which is commonly found in hinge migration kinematics (Fig. 3; for detailed discussion, see Mercier et al. 2007; Tavani et al. 2007).

The present paper presents a fault-related fold case study in the southern Tunisian foreland basin. In this region, the folds have a continuous growth-strata sequence. The study aimed to identify geometrical characteristics that could prove helpful in demonstrating the fold kinematics, as predicted by the fold model. The methods could be adapted and tested on a field scale and generalised for natural case studies of fault-related folds. It is hoped that this work will also stimulate further research by presenting another natural example of growth-strata in a foreland basin.

Typically, growth strata overlay existing sedimentary rocks. For dating tectonic phases, unconformities are traditionally very useful. However, our work on hinge migration shows that the use of unconformities as tectonic markers needs to be reconsidered.

The selected fold structures are located in the Gafsa basin (Atlas Mountains, southern Tunisia). The fold structures are characterised by the following conditions, which proved beneficial to the study:

- A simple contractional deformation: the study area is located in the frontal zone of an orogenic system, characterised by low deformation amplitudes that do not exceed 20 % shortening (Ahmadi 2006).
- Deformation occurred from late Miocene to Recent times (Ben Ayed 1986; Zargouni 1984; Zouari 1995; Bouaziz et al. 2002; Ahmadi et al. 2006).
- The growth strata are relatively thick, with maximum thicknesses of 1,000 m.
- An arid climate results in excellent outcrop conditions. Under these conditions, there is a minimal vegetation cover over the fold cores and fold flanks, facilitating field-data acquisition and satellite-image analysis.
- The Gafsa basin contains many examples of isolated folds that can be used to validate the study observations and findings.

2 Geological setting

2.1 Geodynamic history

The southern Tunisian Atlas is part of the North African Oriental Atlas. It includes the frontal zone between the Oriental Atlas fold belts to the north and the unfolded tabular domain of the Saharan platform to the south (Fig. 4; for a more detailed map of the Tunisian Atlas, see online resource 1). This area is also part of the Gafsa basin, which is known for the phosphate-mining exploitation in the Eocene Metlaoui Group. This basin, in addition to the entire North African margin, is characterised by a continuous and extensive tectonic regime from the Triassic age to the Senonian (Ben Ayed 1986; Zargouni 1984; Ouali 1984, 2007; Bouaziz et al. 2002; Frizon de Lamotte et al. 2000, 2009; Piqué et al. 2002). From the Tertiary to the present, the African–Eurasia tectonic plate collision has generated compressive stress that has led to the creation of the Atlas ranges (Tricart et al. 1994; Ouali 1984, 2007; Outtani et al.

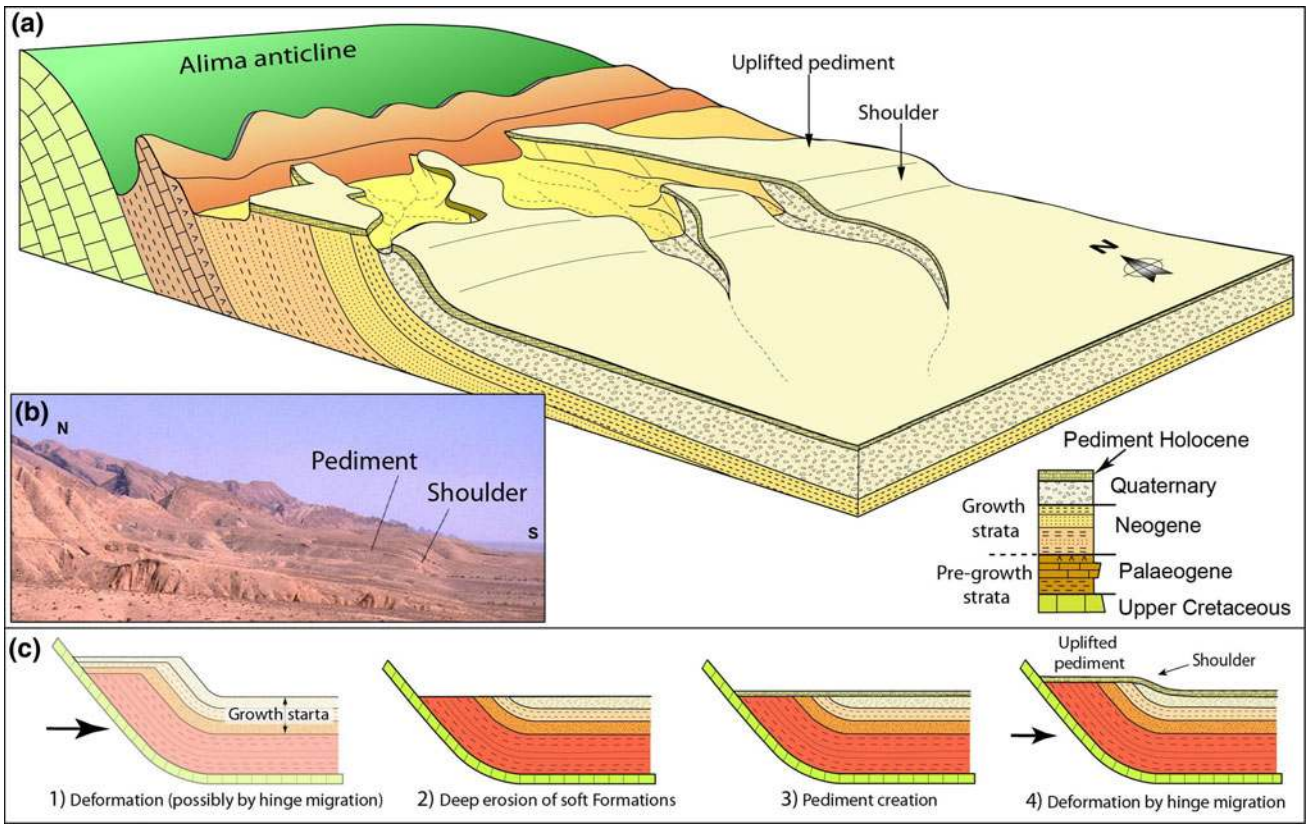

Fig. 3 Growth-strata evidence on the southern flank of Jebel Alima (Gafsa basin, southern Tunisia); the growth strata are represented by Neogene and Quaternary terrestrial sediments (**a**, **b**) but the characteristic geometry of the fold kinematics is observed on the youngest bed, consisting of a late Quaternary pediment dated at 150–160 ka BP (Ben Ouezdou 1994; Swezey 1996). This geometry was interpreted by Ahmadi et al. (2006) as synclinal hinge migration related to a fault-propagation fold (**c**), but there was no evidence of any kinematics on the remaining growth strata

1995; Martinez et al. 1990; Creuzot et al. 1993; Meulenkamp and Sissingh 2003). In the Gafsa basin, compressive tectonics have been detected in the upper Miocene; however, the main phase that was responsible for the actual fold relief occurred during the Quaternary and remains active today (Delteil 1982; Swezey 1996; Letouzeu and Trémolières 1980; Dlala and Hfaiedh 1993; Addoum 1995; Zouari 1995; Bouaziz et al. 2002; Ahmadi 2006).

Following this tectonic history, the Gafsa basin displayed actually two major fault directions:

1. NW–SE faults, such as the Gafsa fault or the Negrine–Tozeur fault;
2. East–West faults that are located beneath East–West fold range (Fig. 4). These faults are actually represented by blind thrusts that were originally normal faults during the Mesozoic age.

In this work, we will focus on two anticlinal structures that are characterized by simple deformation and low erosion. The chosen structures are Jebel Sehib, which is an individual anticline (online resources 2, 3), and Jebel Alima that belongs to the Metlaoui range (Fig. 3).

2.2 Lithostratigraphy

In the Gafsa basin, the stratigraphy is mainly composed of sedimentary series ranging from the Paleozoic to the Quaternary. In this study, outcropping formations that begin with the late Cretaceous Zebbag formation and include recent sediments will be presented (Fig. 5). These formations were divided into two groups: pre-growth strata and growth strata.

2.2.1 The pre-growth strata

- The Zebbag formation (Cenomanian–lower Turonian) consists mainly of claystone at the bottom, interbedded with numerous carbonate and anhydrite horizons.
- The Aleg formation (upper Turonian–lower Campanian) consists of thick local calcareous claystone with thin fossiliferous limestone intercalations.
- The Abiod formation (upper Companian–Maastrichtian) consists of two thick and massive fossiliferous carbonate members (100 m each), separated by a soft

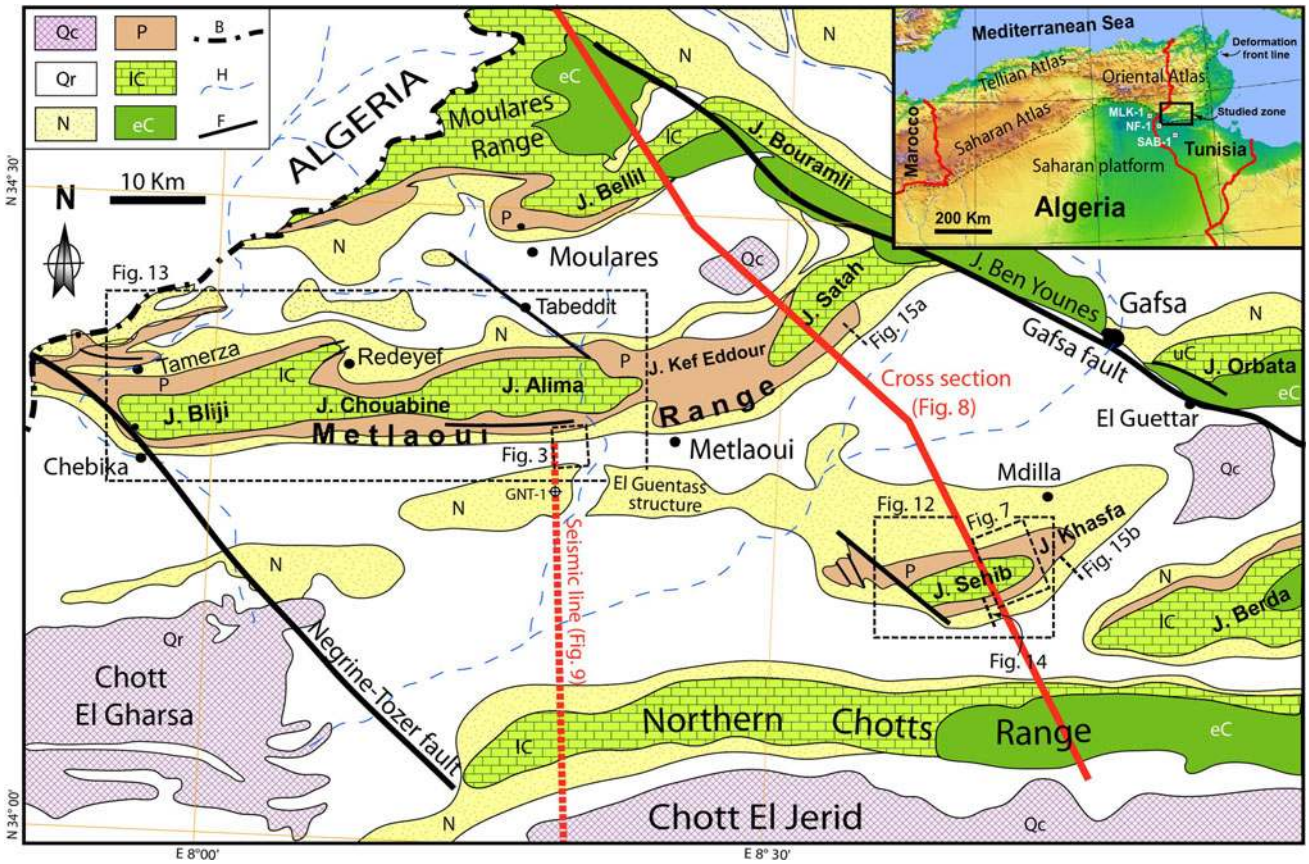

Fig. 4 Simplified geological map of the Gafsa basin showing the locations of the study areas and various text figures (see also online resource 1). *Q* Quaternary Chotts formation, *Qr* Quaternary recent sediments, *N* Neogene, *P* Palaeogene, *lC* late Cretaceous, *eC* early Cretaceous, *B* Tunisian/Algerian border, *H* hydrographic net, *F* fault

middle member (100 m) composed of thin clays, marls, argillaceous limestone and phosphatic limestone intercalations. The top of the upper carbonate member constitutes the core of the Alima and Sehib folds.

– The El Haria formation (Paleocene) consists of mainly calcareous claystone that is 40–60 m in thickness.
– The Metlaoui Group (upper Paleocene–lower Eocene) consists of three formations:
  - Selja formation consists of evaporitic and sallow pelagic sequences composed of clay, fossiliferous dolomite and gypsum from the upper Paleocene to the lower Eocene and ranging from 60 to 80 m in thickness.
  - Chouabine formation (lower Ypresian) is composed of phosphatic limestone and claystone with thicknesses ranging from 10 to 30 m.
  - Kef Eddour formation (upper Ypresian) is composed of one massive fossiliferous limestone package with an average thickness of 40 m.
– The Jebs formation (Lutetian) is composed of white dolomite at the base and massive gypsum beds intercalated with claystone at the top. The thickness ranges from 20 to 60 m.

2.2.2 *The growth-strata*

- The Sehib formation (approximately middle to lower Miocene) is composed of silty and argillaceous sandstone with locally thick conglomerates at the base. The thickness of this formation varies from 0 to 60 m.
- The Beglia formation (middle to late Miocene) is consists of a mainly sandy fluvial formation with some claystone bed intercalations at the top. The thickness varies from 10 to 190 m and is generally thicker to the west.
- The Segui formation (late Miocene to late Quaternary) is mainly composed of sandstone interbedded with siltstone, paleosoils and claystone. The upper part of the formation is dominated by conglomerates and conglomeratic sandstone series. This formation, with a thickness that ranges from 150 to 600 m, constitutes the thickest part of the growth strata.

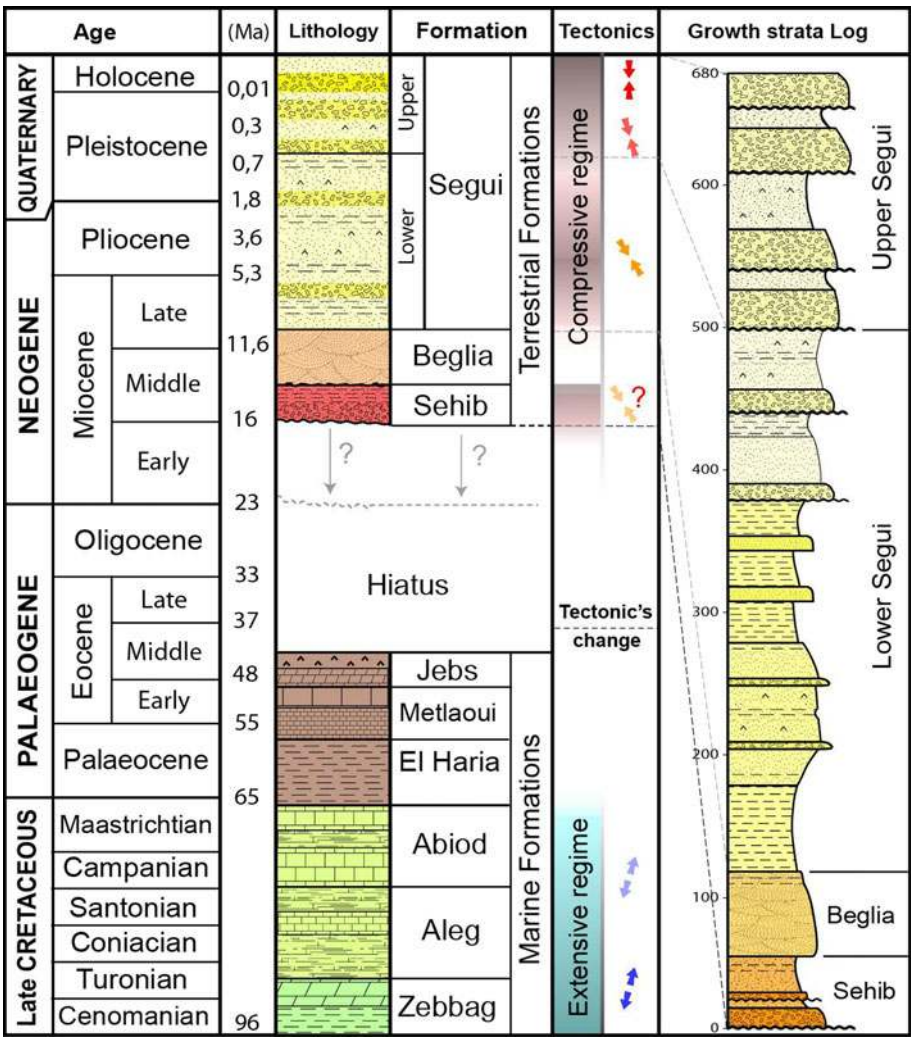

Fig. 5 Lithostraigraphic column of outcropping series in Gafsa basin and detailed log of the growth strata on the southern limb of the Jebel Sehib anticline

The growth strata are made of continental clastic sediments represented by sandstone, siltstone and claystone. If we exclude the Beglia formation, representing an important and permanent fluvial system carrying sediment from the south-west to north-east (Mannaï-Tayech and Otero 2005), all other formations resulted from sedimentation with short-distance transport in episodic flush-flooding fluvial systems, alluvial fans and paleo-soils. In fact, since late Miocene, the local Chott El Gharsa base level was disconnected from the basin and was not affected by eustatic fluctuations (Swezey 1996; Ben Ouezdou 1989; Patriat et al. 2003). Subsequently, sedimentation of the Segui formation was controlled only by climate and tectonics.

Climate changes during late Miocene to Quaternary times were mainly controlled by glaciations (Van Vliet-Lanoë 2005). During glacial periods, climate became drier in Gafsa basin latitudes and all southern Mediterranean regions. This led to evaporitic, matrix-rich sediments with spasmodic encrusted pediments associated with soil erosion. During inter-glacials, the climate became more rainy and suitable for soil accumulation and more active fluvial systems (Fig. 6).

Detailed lithological study based on three logs acquired in southern flanks of the Sehib and Khasfa anticlines showed the intercalation of clastic sediments representing alternating humid and arid climatic conditions (online resource 2). Two specific dry-climate intervals are highlighted in all the logs, almost at the same stratigraphic position, the first located at the base of the Segui formation and the second at the top.

On the other hand, the Mediterranean region suffered two major climatic crises in Neogene time interval. The first corresponds to the Messinian crisis during which the Mediterranean Sea was barred in the Strait of Gibraltar, leading to an important seawater evaporation period and a regional climatic change to drier conditions (Weijermars 1988; Rouchy 1999). The second was recorded during the Villafranchian (Late Pliocene–Early Pleistocene; Combourieu-Nebout et al. 2000) and led to a well-known continental encrusted pediment (Croûte Villafranchienne)

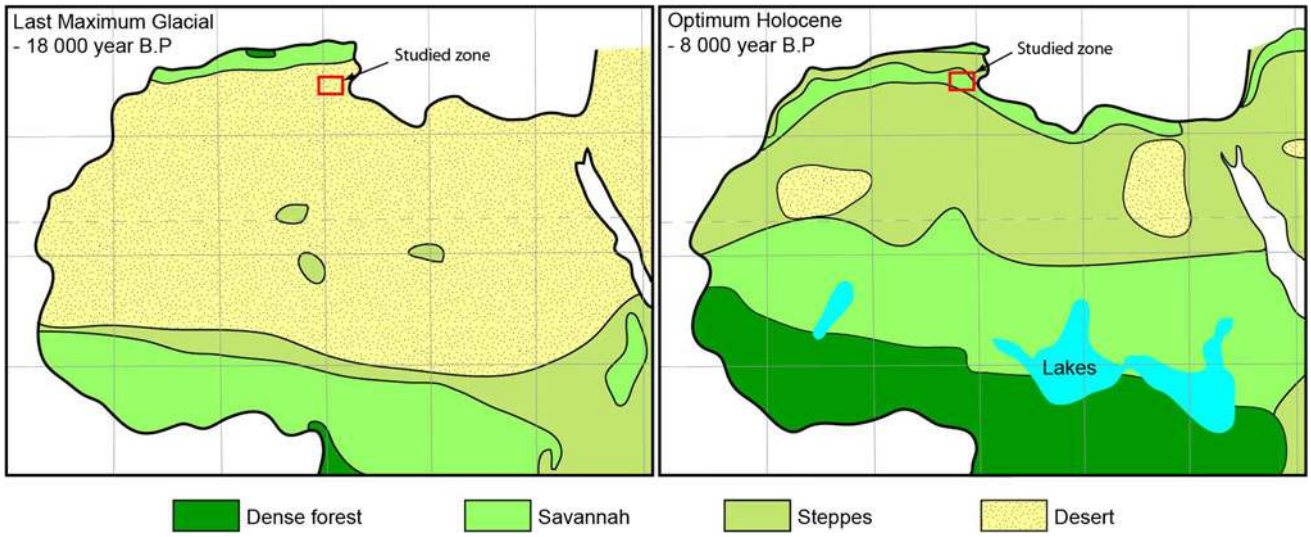

Fig. 6 Vegetation cover of Central and North Africa during last glacial maximum and Holocene climate optimum (adapted after Petit-Maire et al. 1999)

in North Africa and southern European regions. These two major crises, which are contemporaneous with a glacial maximum, can be correlated with the two major periods of arid climatic conditions observed in the Segui formation (late Miocene–Quaternary). The basal one is correlated to Messinian crisis and the second to Villafranchian (online resource 2).

Tectonic compressive activity in the Gafsa basin started in the late Cretaceous and many authors think that it still active today (e.g. Letouzeu and Trémolières 1980; Zouari 1995; Bouaziz et al. 2002). In this period of time two major compressive phases have been highlighted in Tunisia and were responsible for the deformation in the Oriental Atlas. These phases are middle–late Miocene with a shortening direction NW–SE (Patriat et al. 2003; Bouaziz et al. 2002) and post-Villafranchian with shortening close to N–S (Letouzeu and Trémolières 1980; Delteil 1982; Ouali 1984; Zouari 1995; Swezey 1996; Patriat et al. 2003). Both phases were contemporaneous with the deposition of the Segui formation and, considering that eustatism did not control sedimentation (endorheic base level called Chott El Gharsa), tectonic manifestations should be directly correlated with grain size and sequence staking (online resource 2).

The interpretation of the time and amplitude of tectonic activity shows clearly that the main shortening deformation in the Gafsa basin occurred very recently, i.e. during the Quaternary. Three recently deformed pediments (online resource 3) containing old civilisation tools have been dated at 160 ka BP (Ben Ouezdou 1989) and 150 ka BP by U/Th methods (Swezey 1996), indicating that this tectonic activity was very recent and probably still active. However, compressive deformation should begin at least during the deposition of the Sehib formation (middle Miocene or earlier), when thick conglomerates formed for the first time in this basin. Former marine formations, such as the Metlaoui Group or the El Haria formation do not show unconformities, nor significant changes in thickness or facies all over the Gafsa basin. This leads to the conclusion that even though there was a Palaeogene deformation it must have been of very low amplitude.

2.3 Structural features of the Gafsa basin folds

The Gafsa basin folds (e.g. J. Sehib, J. Alima, J. Chouabine, J. Bliji, J. Bellil, J. Satah and the northern Chotts range) are mainly asymmetrical with long, gently-dipping northern limbs (general dip between 10° and 25°N) and steeply dipping southern limbs (dips from 50°S to vertical) The asymmetric geometry of the Gafsa basin folds fits with the fault-propagation fold model as described by Suppe (1983). This model was adopted by Creuzot et al. (1993), Outtani et al. (1995), and Ahmadi et al. (2006) based on fold geometry (Fig. 7). As previously interpreted by Ahmadi (2006), faults with NW–SE strikes function as tear faults by facilitating a differential shortening that increases towards the east in Gafsa basin. E–W striking faults accommodate the compressive deformation along the east–west axis, as exemplified by the Metlaoui range or the Northern Chotts range (Outtani et al. 1995; Ahmadi et al. 2006) and are actually thrust faults which generate all the fault-related folds of Gafsa basin, starting always from the same detachment level located at the base of the Jurassic series or in the Triassic (Fig. 8).

Some authors have proposed that salt tectonics can be used to explain the Gafsa basin anticlines (Hlaiem 1999).

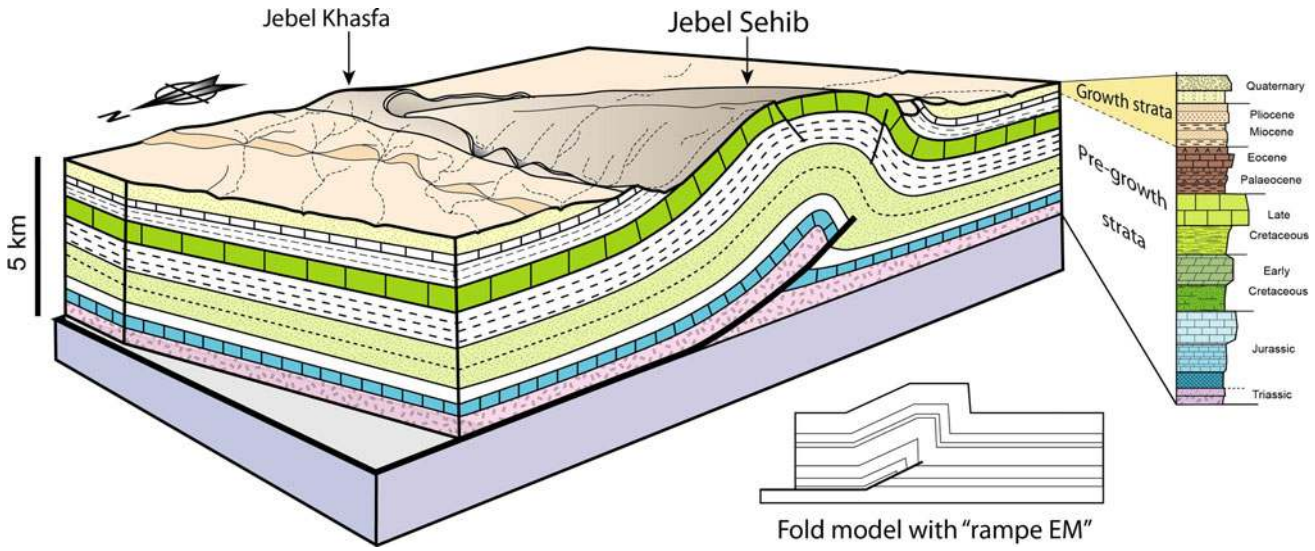

Fig. 7 Block diagram of the Jebel Sehib anticline and its interpretation as a fault-propagation fold using the Rampe EM forward modelling program of Mercier (1995)

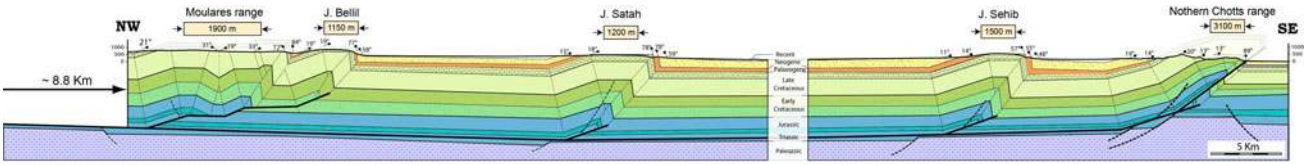

Fig. 8 Geological cross section oriented NW–SE through Gafsa basin (for location, see Fig. 4). The horizontal shortening of the different fault-propagation folds splaying off the main decollement is noted above each structure, giving a total shortening of the whole section of 8.8 km

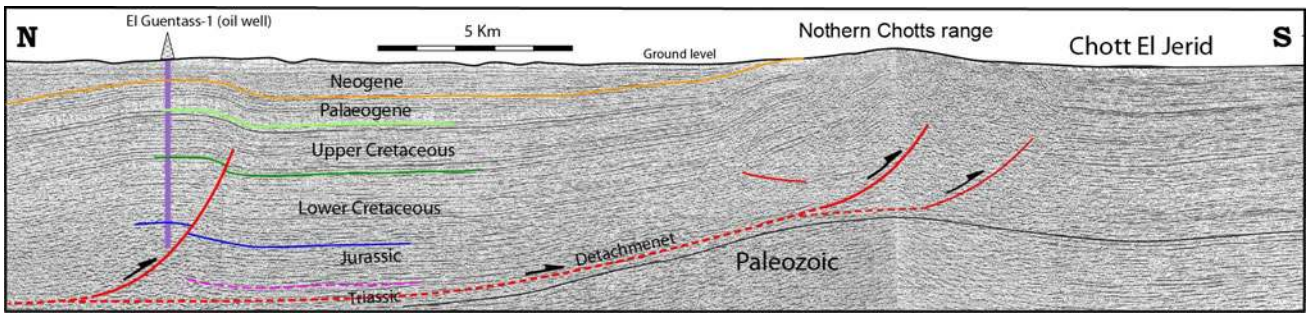

Fig. 9 Seismic line across El Guentass structure and northern Chotts range (for location, see Fig. 4). Reflectors in El Guentass structure show a fault-propagation fold with no evidence of salt movement in the core. In the northern Chotts range, poor seismic quality is not clear enough to identify any salt tectonics. Moreover, this profile is obtained by splicing two lines in the northern Chotts range, and border effects make it hard to interpret

However, oil wells drilled in the basin show that this cannot be involved. The Sabria-1 (SAB-1) and Nafta-1 (NF-1) wells located to the south and southwest of the study area (Fig. 4) showed salt cumulative thicknesses of >50 m. To the west, in Chott Melkhir-1 well (MLK-1), late Triassic evaporite interval is around 400 m thick and contains salt, anhydrite, dolostone and claystone intercalations. This salt budget is too thin to generate halokinesis. In the same way, seismic lines across the El Guentass well and the northern Chotts range do not show any clear evidence of salt movement (Fig. 9). A recent field gravimetric study (Riley et al. 2011) proved that there was no evidence of a negative gravity anomaly in the Alima anticline and therefore no possible salt intrusion in the core of the fold. Moreover, other than with Gafsa fault-related structures, field data in the Gafsa basin folds do not show any field arguments in favour of salt tectonics, such as radial extensive faults, thickness changes, rim synclines or any

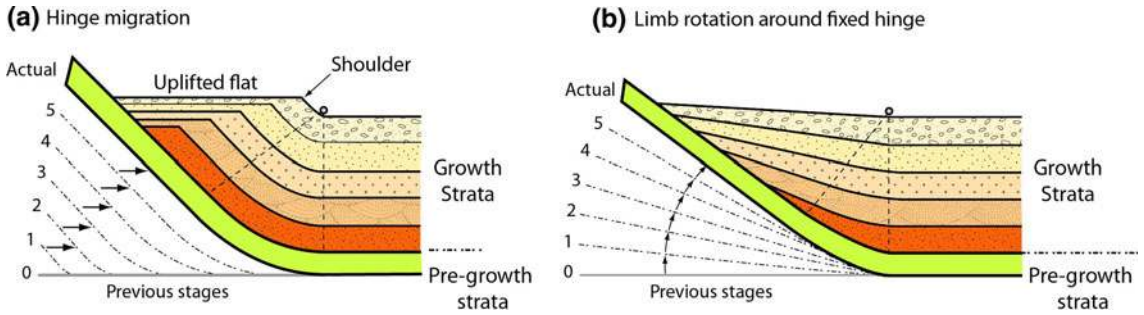

Fig. 10 Expected geometry in growth strata obtained with different hinge kinematics **a** with hinge migration, **b** with limb rotation around fixed hinges (adapted from Rafini and Mercier 2002). *Lines 1–5* show schematically the evolution of the fold limb in the pre-growth strata

other sedimentological phenomena like those observed in the central Tunisian folds located north of the studied region.

A second hypothesis explains fold generation as a consequence of basement strike-slip movements (Swezey 1996; Ben Ayed 1986; Zargouni 1984; Bouaziz 1995; Riley et al. 2011). However, the frontal zone between tabular Saharan platform and folded Atlas domains is an oblique NW–SE line passing to the west of our study area. If there was any significant strike-slip movement along a basement fault is this region one would expect the development of a deep NW–SE trending basin (graben, half-graben or pull-apart) at the same time (cf. online resource 1). None of the geological maps show any extensional movement above NW–SE faults. On the contrary, the Gafsa fault which has a NW–SE strike, is associated with compressive deformation.

On the Alima anticline cross section, the northern flat plains are in a higher position than the flat plains in the south, a fact used to support the idea of basement-involved deformation. However, the altitude difference (200–300 m) is too insignificant to explain the fact that the actual observed deformation is >1,500 m in the Alima anticline. The Beglia formation (Middle–Late Miocene) was deposited in a permanent fluvial system carrying sediments on a regional scale from the south-west to the north-east. This means that topography was almost flat at that time or having a general very gentle slope towards NE (flow direction). So the actual observed difference between altitudes was effectively acquired during a deformation post-dating the late Miocene. Although basement wrench fault models can be applied, it is unlikely that basement wrench faults are major contributors to the actual anticline structures. Hence we still believe that differential layer parallel shortening (LPS) could be the main source of this cover thickening.

The establishment of a particular fold model cannot be solely based on geometric analogy but instead requires further arguments that particularly relate to the kinematics of folding. This paper explores the growth-strata method that could provide information about previous fold geometry stages. In the study basin, growth strata are quite thick and continuous. This particularity is mainly because the growth strata in the Gafsa basin are related to the tectonic uplift. In fact, the drainage net in this region has been driven to the endorheic Chott El Gharsa from Miocene to present times (Ben Ouezdou 1989; Patriat et al. 2003). During this period, the Gafsa basin was disconnected, and eustatic fluctuations occurred that caused the equilibrium profile and accommodation to be controlled only by the tectonics.

3 Growth-strata geometry

3.1 Theoretical concept

The growth-strata geometry has been used to differentiate hinge kinematics. Fixed hinges detachment folds are disharmonic folds that can be primarily characterised by limb rotation around fixed hinges. There are few examples of detachment folds (e.g. Epard and Groshong 1995); however, mobile hinges are usually related to fault-related folds (Homza and Wallace 1995; Epard and Groshong 1995; Poblet and McClay 1996; Storti and Poblet 1997; Salvini and Storti 2002). The different geometries of the growth strata developing during hinge migration, as opposed to limb rotation around a fixed hinge are shown in Fig. 10.

This method has been used for some natural cases where folds were still immersed in the sediments, such as subsea folds that can be studied using seismic profile data. In nature, there exist few examples that illustrate the geometry of growth-strata. Most of the studies that have been performed are incomplete (generally focused on one flank) and do not demonstrate the relationship between growth-strata geometry and the fold model. The reason for this is that the most interesting geometric details are generally located next to the fold, which subjects them to deep erosion on outcropping folds

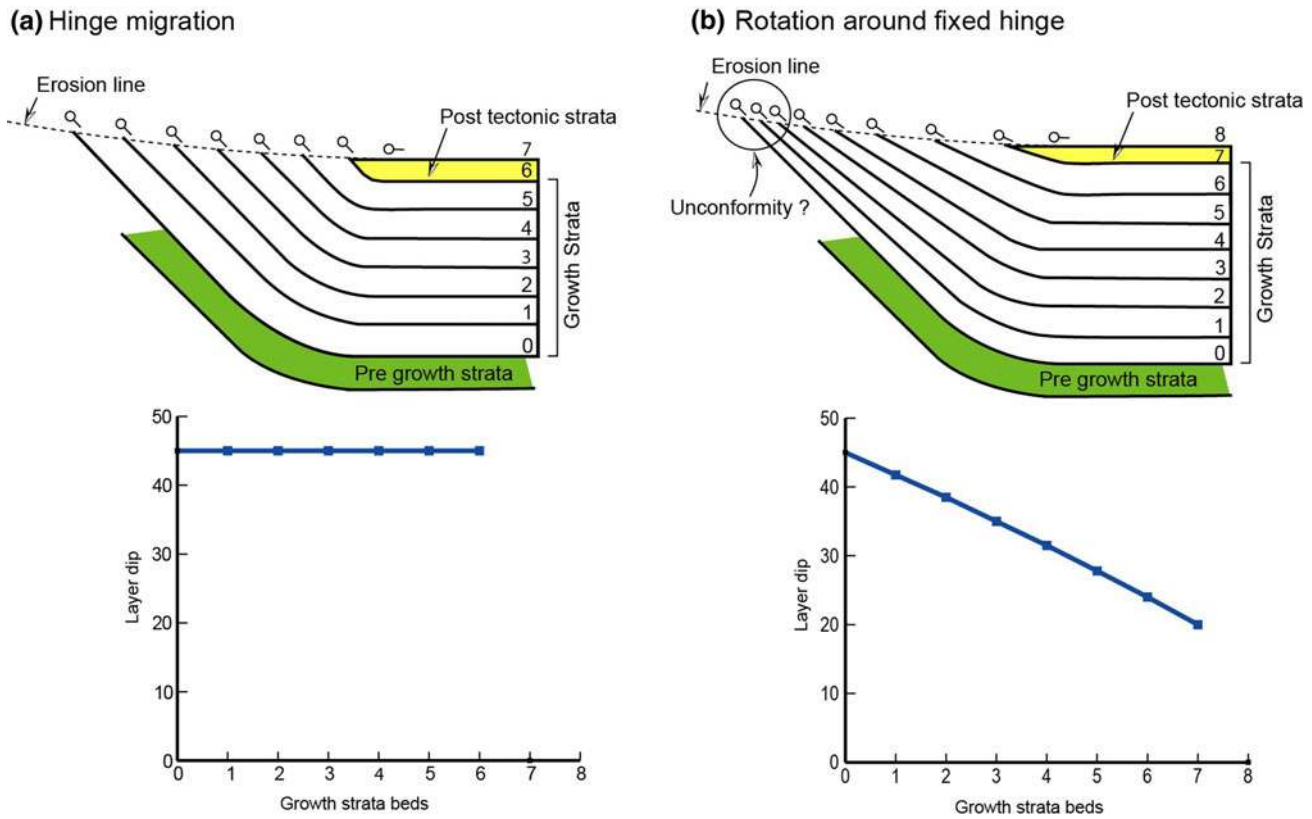

Fig. 11 Dip trend lines of growth-strata layers in deep erosion cases **a** with hinge migration, **b** with limb rotation around fixed hinges

(complete discussion in Mercier et al. 2007). To resolve this problem, deep erosion cut-off lines were imposed in the original Rafini and Mercier (2002) model. The results (Fig. 11) indicate that it remains very difficult to detect the difference between the two kinematic models in the field on this basis, because the difference in dips is too small to be distinguished in field measurements (or by the naked eye on constructed profiles, e.g. the circle mark in Fig. 11b). However, by utilising a graph that plotted growth-strata layer dips versus bed numbers or thickness, the difference between the models (hinge migration and limb rotation) can be discerned. The hinge migrating case is characterised by constant growth-strata layer dips, even in the most recent layers (Fig. 11a), whereas the flank rotation model shows progressive decrease in layer dips as one approaches the hinge line (Fig. 11b).

3.2 Geometry of growth-strata in Sehib and Alima anticlines

The Jebel Sehib case study shows complete growth-strata sedimentation from the Miocene to the present time (growth-strata log in Fig. 5). The geological map of Jebel Sehib displays an important unconformity on the northern limb of the anticline (Fig. 12). The sands and conglomerates of the upper Segui formation overlap the lower Segui sands, which is the case for almost all of the Neogene sediments and locally late Eocene formations. An interesting point is that this unconformity disappears completely on the entire southern limb, where the same upper Segui series are in perfect conformity on top of the lower Segui. The same geometry is observed in the Alima anticline (Fig. 13). On both limbs, water wells exploiting water from the Miocene sand reservoirs (lower Segui and Beglia formations) assisted in developing cross sections below the topography.

This observation is puzzling because unconformities are supposed to be isochronous, especially in the same fold structure, and therefore this type of geometry is typically used for the dating of tectonic events. In the cases described above, this interpretation is not plausible because of apparently non-isochronous unconformity.

3.3 Growth-strata dip evolution

In the Gafsa basin case study, the growth-strata sediments are from the Neogene terrestrial series, which consist mainly of loose to friable sands, conglomerates, siltstone and poorly compacted sandy claystone. The equilibrium

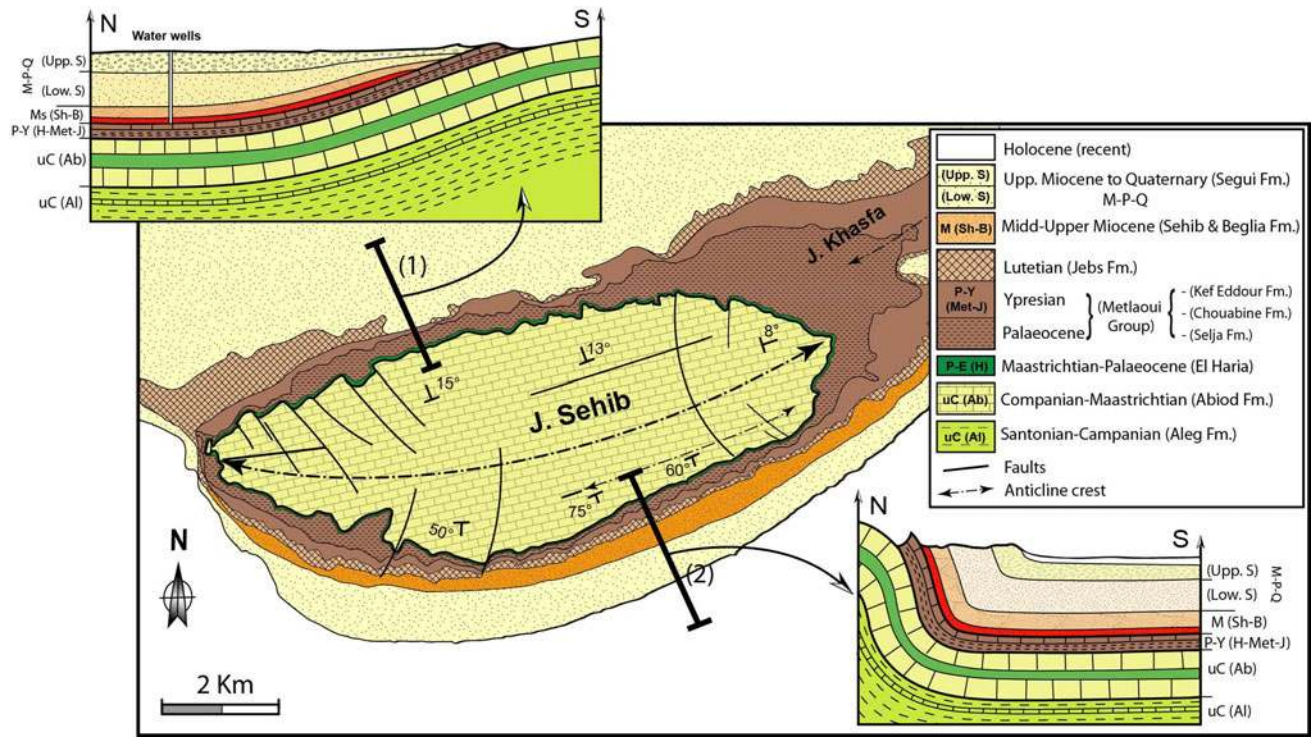

Fig. 12 Geological map of the Jebel Sehib anticline and cross-sections showing the growth-strata geometry on the northern and southern limbs. Note that the Segui formation (Mio–Plio–Quaternary) on the northern limb overlays with unconformity all Neogene sediments and some Palaeogene sediments. This unconformity is absent in the southern limb. *S* Segui Fm, *Sh* Sehib Fm (*red layer*), *B* Beglia Fm, *Ab* Abiod Fm and *Al* Aleg Fm

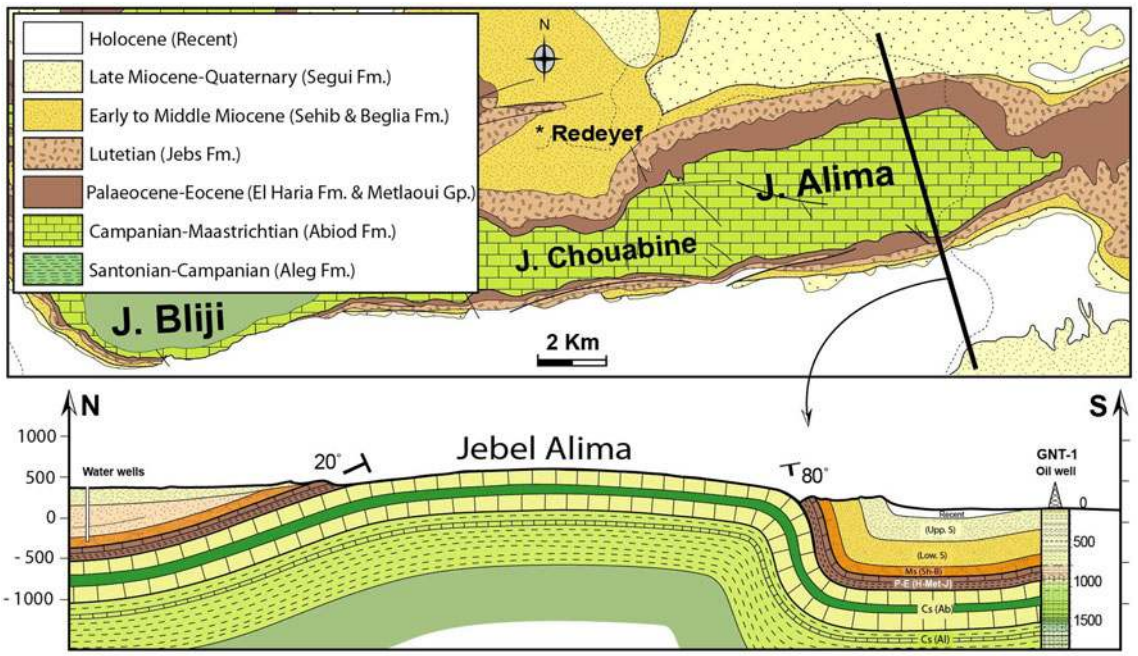

Fig. 13 Geological map and cross-section across the Jebel Alima anticline and its Miocene to Quaternary growth strata

cut-off profile matures very quickly as these sediments erode, which obliterates any markers that could be used to characterise the hinge kinematics (cf. Fig. 10).

The method described in Fig. 11, which showed that hinge migration results in a constant dip trend line through the growth strata, has been applied to several Gafsa basin

anticlines, with particular focus on the Jebel Sehib case (Fig. 12). On the southern limb, the Segui formation is in perfect conformity with each of the series including the lowermost beds of the growth-strata (Sehib formation). The underlying pre-growth strata have an average dip of 50°S. At the top of the growth-strata, very recent pediments have been dated as forming 150 ka BP (Swezey 1996) and now display the same dip values (58°S in Fig. 14) as displayed by the pre-growth strata. Although the measurements show some variation (between 45° and 60°), the overall trend line through the measured dips is clearly horizontal, indicating a constant dip of about 54°–55°S (Fig. 14).

In other Gafsa basin anticlines, the same constant dips were observed on the southern limb in the growth-strata beds (Fig. 15), as predicted by the hinge migration model (Rafini and Mercier 2002).

4 Comparison of the field data with a numerical model

The growth-strata geometry of several folds of the Gafsa basin show unconformities on the gently-dipping northern limbs and constant bed dips on the steeply-dipping southern limbs. This geometry is difficult to explain with the concept of folding with a fixed hinge. In fact, this concept stipulates that folds are older than the most recent undeformed layer, which, in this case, is the upper Segui formation on the northern limb. What then accounts for the

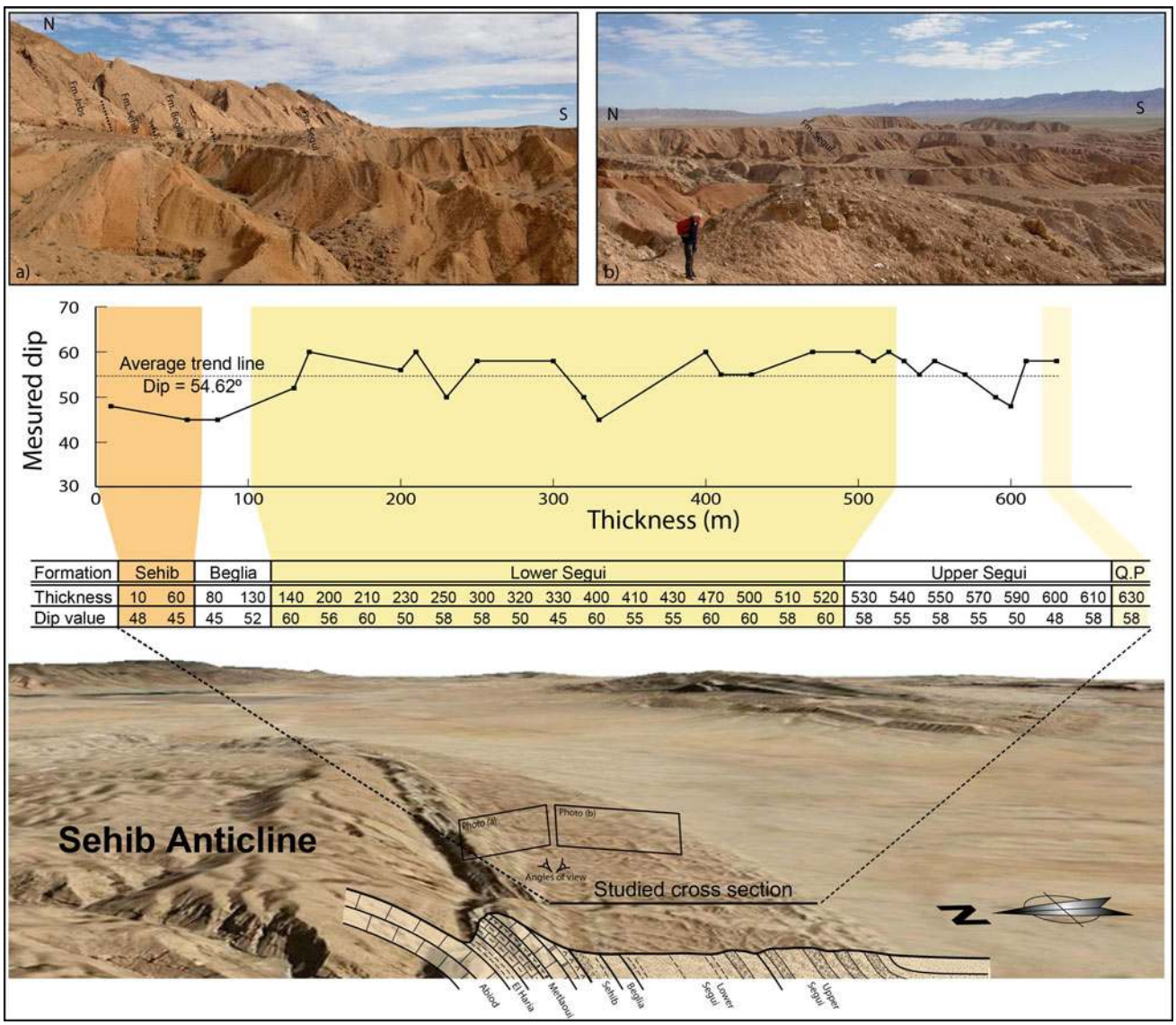

Fig. 14 Dip evolution of growth-strata beds on the southern limb of Jebel Sehib, from the late Cretaceous Sehib formation to the Quaternary pediments (QP) The 3D eastward looking satellite image (*below*) was obtained from Google Earth, and shows the position of the two ground images (*above*)

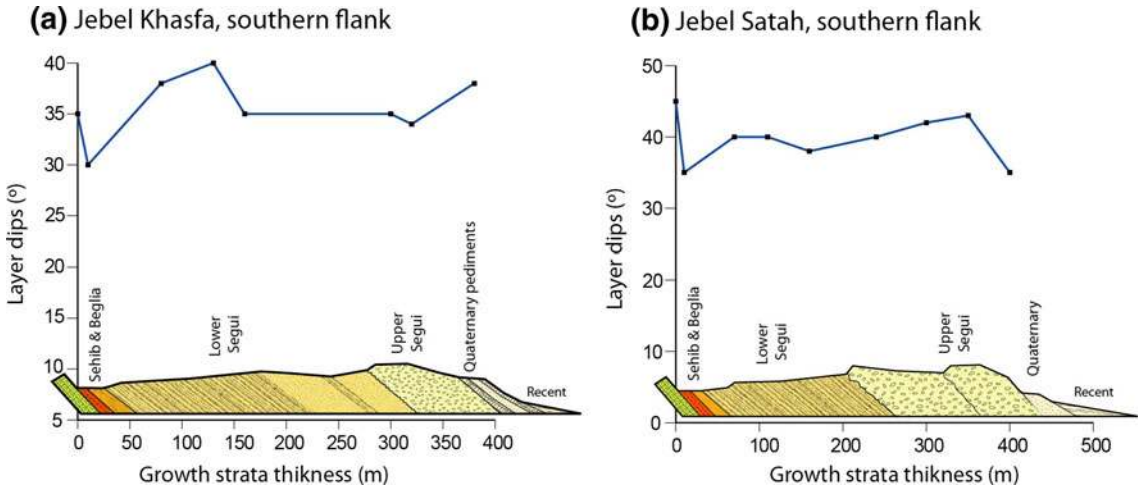

Fig. 15 Dip trends of growth-strata bedding in other southern flanks of Gafsa basin folds **a** Jebel Khasfa, **b** Jebel Satah. Both examples show *horizontal trend lines*, confirming the general constant dip of all growth-strata beds, including recent sediments

deformation in the same beds on the southern limb, which are clearly involved in the folding? Limb rotation cannot explain this natural example, and it is concluded that fixed hinges are not the correct kinematics for the Jebel Sehib folding and the other folds described above.

In order to explore the fold mechanism further, numerical forward modelling has been used. The modelling is based on the fault-propagation fold model, and is associated with ideas on growth-strata sedimentation that is founded in the work of Rafini and Mercier (2002). The geometrical parameters that were used are similar to those in the initial model of Jebel Sehib (Fig. 7), and the sedimentation and shortening rates were adapted to fit to the actual growth-strata geometry that was observed in the cross-sections (Fig. 12). The fault-propagation fold model assumes hinge migration kinematics in both of the peripheral kinks where growth-strata are deposited. The resulting model (Fig. 16) clearly shows immerged growth-strata sediments on the back limb (northern limbs on the anticlines studied in the Gafsa basin) and emerged growth-strata ends on the forelimb (southern limbs of the anticlines studied).

The model distinguishes two different geometrical relationships between pre-growth strata and growth strata. On the back limb, growth-strata beds are onlapping the pre-growth beds. With some erosion cut-off, these onlaps can become top laps in their uppermost parts (Fig. 16). In the forelimb, growth strata emerge from the basin due to higher uplift rates in the forelimb than in the back limb. As a result, no contacts are made with the post-growth strata in the vicinity of the fold. This geometry is termed offlap.

To obtain different relationship geometries in the limbs of similar anticline structures, characterised by immerged growth strata or onlaps (top laps with erosion) on one side of the fold and emerging growth-strata or off laps on the other side of the fold, a differential uplift rate needs to be used. The uplift amplitude is only dependent on the deformation rate and the limb dip. When the sedimentation rate is greater than the uplift rate, the growth strata will cover the older sediments unconformably. However, when the sedimentation rate is lower than the uplift rate, the emerging series (offlaps) will show consistency with the growth-strata. The uplift rate is dependent on the shortening rate and the limb dip. Because the dips on fold limbs are different for most fault-propagation folds, only a comparison of shortening rates can be made, which remain constant for each fold. In this study, only the shortening rate was used to quantify the deformation, and the uplift rate was independently calculated for each limb.

In our case study, the estimated sedimentation-to-shortening rate ratios resulted in an uplift rate that was greater than the sedimentation rate in the forelimb (southern steeply-dipping limb) and an uplift rate that was lower than the sedimentation rate in the back limb (northern gently-dipping limb). In general, the ramp dips of fault-propagation folds varied from 20° to over 50° in most cases. The graph (Fig. 17) of plotted sedimentation and shortening ratios versus back limb dips facilitates the prediction of emerging growth-strata from the basin (offlaps) or immerged growth-strata (onlaps) for the fold propagation fold flanks. Each line on the graph characterises the limit at which the growth-strata geometry changed from emerged (below the line) to immerged (above the line). The special area between both lines defines the ratios (sedimentation-to-shortening) and the ramp dips that yield different growth-strata geometry on both limbs, as in the case of the present study. The solid curve (back limb) was plotted by using the ramp dips. The dashed curve

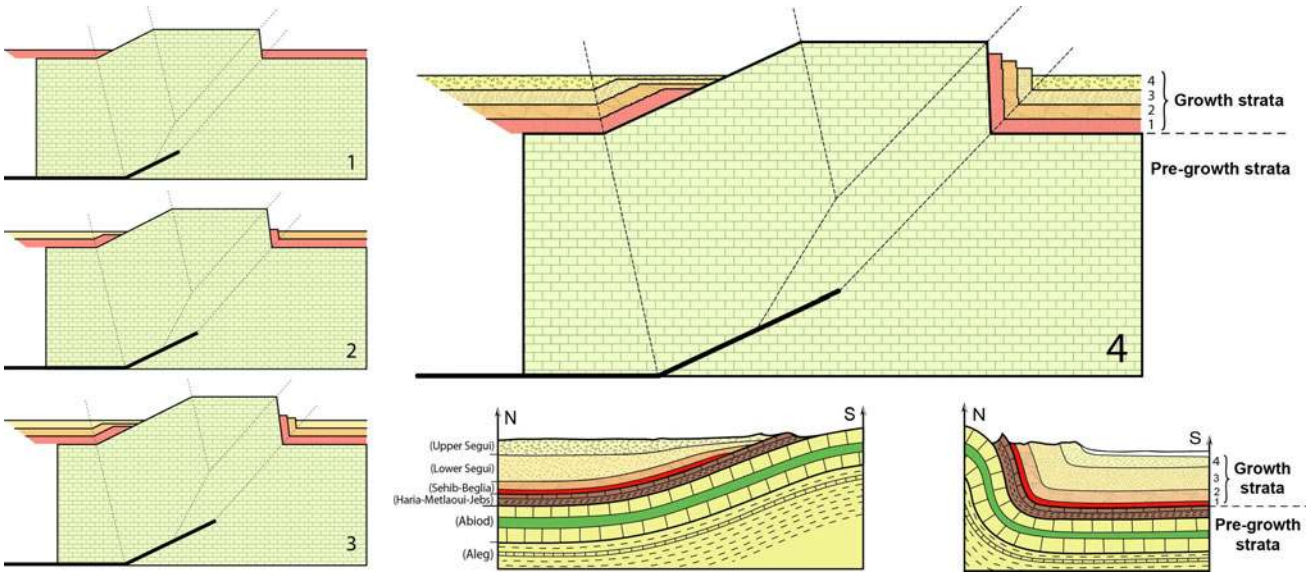

Fig. 16 Fault-propagation fold associated with growth-strata modelled (stages **1**–**4**) in relation to the real structure geometry of the Jebel Sehib anticline (*below right*, cross-sections taken from Fig. 12). The modelling of the sequence of stages is adapted to the estimated sedimentation and uplift rates, using software derived from Rafini and Mercier (2002)

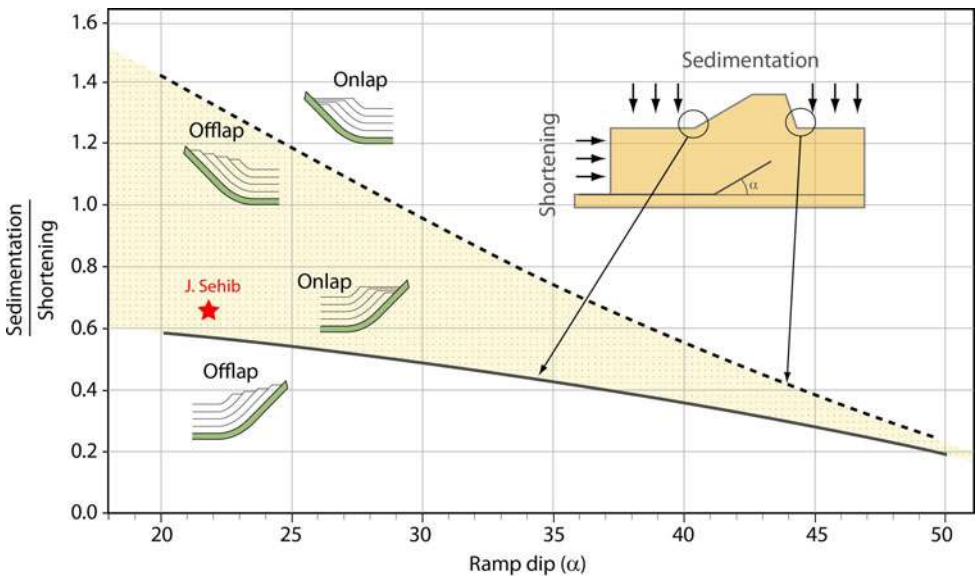

Fig. 17 Graph of the ratio sedimentation rate to uplift rate in relation to the dip of the ramp fault. The graph predicts the growth-strata geometry on limb onlaps and limb offlaps. The *dashed line* represents the steeply-dipping forelimb and the *full line* represents the gently-dipping back limb of the fault-propagation fold. In the case of the Jebel Sehib anticline, the plot of estimated sedimentation-to-shortening ratio is located in the *shaded area*, which confirms the mixed growth-strata geometry which was observed (for explanation, see text)

represents the forelimb dip of the fault-propagation fold (southern limb in this case study) and was computed using the back limb dip. The angle "α" defines both the ramp dip (the dip of the fault splaying up from the detachment, Figs. 16, 17) and the back limb dips. For this angle, there was a single solution for the forelimb dip. Based on this graph and the field data (geometry of growth strata and ramp dip), an even sedimentation rate of the basin growth-strata or the shortening rate was obtained.

The main concern with this method is that the sedimentation-to-shortening ratio is assumed to be constant, whereas sedimentation rates and deformation rates are not constant in nature. As previously concluded by Rafini and Mercier (2002), the case study also concludes that, in continental domains, tectonic uplifts are correlated to growth-strata sedimentation by the erosion process. The study also supports the notion that when deformation increases, the sedimentation rates proportionally increase.

Climatic correlation leads to a precise dating of the clastic and unfossiliferous rocks of the Segui formation. Based on this correlation, we conclude that many low-amplitude deformations took place during late Miocene and Pliocene times but that the main tectonic phases occurred during the Quaternary (post-Villafranchian). This

deformation may still be active, considering the very recent pediment deformation (Fig. 3; online resource 3). This conclusion is specific to the studied anticlines (particularly Sehib and Khasfa) and cannot be generalized over the entire basin because sediments are mainly deposited in proximal alluvial fan systems and consequently reveal only local deformation stages. However, even though this dating method, based on climatic correlation, seems to be consistent and reproducible in several locations of Gafsa basin (Ahmadi 2006), it still needs to be confirmed with an absolute dating method.

5 Conclusions

Classically, growth strata are deposited in anticline footwalls and have fan geometry unconformities that attest syntectonic sedimentation. This study demonstrated that progressive fan unconformities are possible only if hinges are fixed during anticline deformation by flank rotation. The growth-strata geometry of several anticlines of Gafsa basins have been studied in relation to the fold models. These folds have a simple steep fault-propagation fold geometry, as originally described by Suppe (1983) and are assumed to grow by hinge migration. Through the use of forward modelling, asymmetrical unconformities were observed on the limbs of the anticlines and obtained with the fault-propagation fold model that assumed growth-strata sedimentation. The results confirm that folds grow by hinge migration, as predicted by the fold model. This particular geometry can be obtained only in narrow domains of the ratio of sedimentation rate to shortening rate. After the work by Shaw and Suppe (1994), several authors have proposed the use of growth-strata geometry to validate fold kinematics. However, there are few areas in the world that allow a complete study of growth strata on both limbs of individual fault-propagation folds, as presented here.

Acknowledgments This work has benefitted greatly from the programme of the Comité Mixte de Cooperation Universitaire (CMCU) established between French and Tunisian universities. Our thanks go to Jean-Luc Epard and Adrian Pfiiffner for commenting an early draft of this manuscript, and to Farhat Rekhiss and an anonymous reviewer for carrying out thorough reviews and for constructive comments which contributed to an improvement of the final version.

References

Addoum, B. (1995). L'Atlas Saharien Sud-oriental: Cinématique des plis-chevauchements et reconstitution du bassin du Sud-Est Constantinois (confins algéro-tunisiens). Thèse de Doctorat ès Science, Université de Paris XI Orsay.

Ahmadi, R. (2006). Utilisation des marqueurs morphologiques, sédimentologiques et microstructuraux pour la validation des modèles cinématiques de plissement. Application à l'Atlas méridional tunisien. PhD Sciences de la Terre, Faculté des Sciences et Technique de Nantes, Université de Nantes.

Ahmadi, R., Ouali, J., Mercier, E., Mansy, J. L., Van Vliet Lanoë, B., Launeau, P., et al. (2006). The geomorphologic imprints of hinge migration in the fault-related folds. A case study in southern Tunisian Atlas. *Journal of Structural Geology, 28*, 721–728.

Ben Ayed, N. (1986). Évolution tectonique de l'avant-pays de la chaîne alpine de Tunisie du début du Mésozoïque à l'Actuel. Thèse d'État, Université Paris 11.

Ben Ouezdou, H. (1989). Sur l'hypothèse de la mer saharienne Quaternire: analyse du contexte géomorphologique et géologique de l'évolution récente des chotts algéro-tunisiens et du seuil d'Ouedref. *Compte Rendue de l'Académie des Sciences, Paris, T 308*(II), 767–772.

Ben Ouezdou, H. (1994). La partie méridionale des steppes tunisienne. Etude géomorphologique. Thèse Doctorat d'Etat en Géographie Physique, Faculté des Sciences Humaines et Sociales, Univercité de Tunis I, Tunis.

Bernal, A., & Hardy, S. (2002). Syn-tectonic sedimentation associated with three-dimensional fault-bend fold structure: a numerical approach. *Journal of Structural Geology, 24*, 609–635.

Bouaziz, S. (1995). Etude de la tectonique cassante dans la Plateforme et l'Atlas Saharien (Tunisie méridionale): Evolution des paléochamps de contraintes et implications géodynamiques. Thèse de Doctorat Es-Scienceis, Faculté des Scinece de Tunis, Univercité de Tunis II.

Bouaziz, S., Barrier, E., Soussi, M., Turki, M. M., & Zouari, H. (2002). Tectonic evolution of the northern African margin in Tunisia from paleostress data and sedimentary record. *Tectonophysics, 357*, 227–253.

Combourieu-Nebout, N., Fauquette, S., & Quézel, P. (2000). What was the late Pliocene Mediterranean climate like: a preliminary quantification from vegetation. *Bulletin de la Société Géologique de France, 171*, 271–277.

Creuzot, G., Mercier, E., Ouali, J., & Tricart, P. (1993). La tectogenèse atlasique en Tunisie centrale: Apport de la modélisation géométrique. *Eclogae Geologicae Helvetiae, 86*(2), 609–627.

Delteil, J. (1982). Le cadre néotectonique de la sedimentation plioquaternaire en Tunisie centrale et aux îles Kerkennah. *Bulletin de la Société Géologique de France, 2*, 187–193.

Dlala, M., & Hfaiedh, M. (1993). Le séisme du 7 Novembre 1989 à Metlaoui (Tunisie Méridionale): une tectonique active en compression. *Compte Rendu de l'Académie des Sciences Paris, 317*(II), 1297–1307.

Epard, J. L., & Groshong, R. H, Jr. (1995). Kinematic model of detachment folding including limb rotation, fixed hinges and layer-parallel strain. *Tectonophysics, 247*, 85–103.

Ford, M., Williams, E. A., Artoni, A., Vergès, J., & Hardy, S. (1997). Progressive evolution of a fault-related fold pair from growth-strata geometries, Sant Llorenç de Morunys, SE Pyrenees. *Journal of structural Geology, 19*(3-4), 413–441.

Frizon de Lamotte, D., Leturmy, P., Missenard, Y., Khomsi, S., Ruiz, G., Saddiki, O., et al. (2009). Mesozoic and Cenozoic vertical movements in the Atlas system (Algeria, Morocco, Tunisia): an overview. *Tectonophysics, 475*, 9–28.

Frizon de Lamotte, D., Saint Bezar, B., Bracene, R., & Mercier, E. (2000). The two main steps of the Atlas building and geodynamics of the western Mediterranean. *Tectonics, 19*(4), 740–761.

Grando, G., & McClay, K. (2004). Structural evolution of the Frampton growth fold system, Atwater valley-southern Green Canyon area, deep water Gulf of Mexico. *Marine and Petroleum Geology, 21*, 889–910.

Hardy, S. (1997). A velocity description of constant-thickness fault-propagation folding. *Journal of Structural Geology, 19*(6), 893–896.

Hardy, S., & Poblet, J. (1994). Geometric and numerical model of progressive limb rotation: in detachment folds. *Geology, 22*, 371–374.

Hlaiem, A. (1999). Halokinisis and structural evolution of the major features in eastern and southern Tunisian Atlas. *Tectonophysics, 306*, 79–95.

Homza, T. X., & Wallace, W. K. (1995). Geometric and kinematic models for detachment folds with fixed and variable detachment depths. *Journal of Structural Geology, 17*, 575–588.

Letouzeu, J., & Trémolières, P. (1980). Paleostress fields around the Mediterranean since the Mesozoïc derived from microtectonics: comparison with plate tectonics data. In: Edition du Bureau de Recherches Géologiques et Minières (BRGM), 26ème Congrès Géologique International, Colloque CS, pp. 261–268.

Livio, A., Berlusconi, A., Alessandro, M., Michetti, A., Sileo, G., Zerboni, A., et al. (2009). Active fault-related folding in the epicentral area of the December 25, 1222 (Io = IX MCS) Brescia earthquake (northern Italy): seismotectonic implications. *Tectonophysics, 476*, 320–335.

Mannaï-Tayech, B., & Otero, O. (2005). Un nouveau gisement miocène à ichthyofaune au sud de la chaîne des Chotts (Tunisie méridionale). Paléoenvironnement et paléobiogéographie. *Comptes Rendus Palevol, 4*, 405–412.

Martinez, C., Andrieux, J., Truillet, R., & Ben Jemiaa, M. (1990). Les structures synsédimentaires miocènes en compression associées au décrochement dextre Mrhila-Chérichira (Tunisie oentrale). *Bulletin de la Société Géologique de France, 10*, 141–161.

Mercier, E. (1995). *Les plis de propagations de rampes: cinématique, modélisation et importance dans la tectogenése. Habilitation à diriger les recherches*. Univercité de Cergy-Pontoise

Mercier, E., Rafini, S., & Ahmadi, R. (2007). *Folds kinematics in "folds and thrust belts" The "hinge migration" question. A review. Thrust belts and foreland basins part IV. Structural modeling/restoration*. Berlin: Springer.

Meulenkamp, J. E., & Sissingh, W. (2003). Tertiary palaeogeography and tectonostratigraphic evolution of the Northern and Southern Peri–Tethys platforms and the intermediate domains of the African–Eurasian convergent plate boundary zone. *Palaeogeography Palaeoclimatology Palaeoecology, 196*, 209–228.

Muller, K., & Suppe, J. (1997). Growth of Wheeler Ridge anticline, California: geomorphic evidence for fault-bend folding behaviour during earthquakes. *Journal of Structural Geology, 19*(34), 383–396.

Ouali, J. A. (1984). Structure et géodynamique du chaînon Nara-Sidi Khalif (Tunisie centrale). *Bulletin des Centres de Recherches Exploration (Elf-Aquitaine, Pau), 9*, 155–182.

Ouali, J. A. (2007). *Importance du réseau rhégmatique dans la tectogenèse de la Tunisie atlasique à travers l'étude de l'axe Nord-Sud*. Tunis: HDR, Université de Tunis, El Manar Faculté des Sciences de Tunis.

Outtani, F., Addoum, B., Mercier, E., de Frizon Lamotte, D., & Andrieux, J. (1995). Geometry and kinematics of the south Atlas front, Algeria and Tunisia. *Tectonophysics, 249*, 233–248.

Patriat, M., Ellouze, N., Dey, Z., Gautier, G. M., & Ben Kilani, H. (2003). The Hammamet, Gabés and Chotts basins (Tunisia): a review of the subsidence history. *Sedimentary Geology, 156*, 241–262.

Petit-Maire, N., Bouysse, P., De Beaulieu, J.L., Boulton, N.G., Iriondo, M., Kershaw, P., Lisitsyna, O., Partridge, T., Pflaumann, U., Sarnthein, M., Schulz, H., Soons, J., Van Vliet-Lanoë, B., Yuan, B., Guo, Z., Van Der Zijp, M., Atalay, I., Kuzucuoglu, C., Lezine, A.M., Zhuo, Z., Porter, S., Runge, J. (1999). Cartes des environnements du monde pendant les deux derniers extrêmes climatiques: 1- Le dernier maximum glacière (ca 18000 +- 1000 ans B.P); 2- L'optimum holocène (ca 8000 +- 1000 ans B.P.). Commission de la carte géologique du monde, France.

Piqué, A., Tricart, P., Guiraud, R., Laville, E., Bouaziz, S., Amrhar, M., et al. (2002). The Mesozoic–Cenozoic Atlas belt (North Africa): an overview. *Geodinamica Acta, 15*(3), 185–208.

Poblet, J., & Hardy, S. (1995). Reverse modelling of detachment folds; application to the Pico del Aguila anticline in the South Central Pyrennes (Spain). *Journal of Structural Geology, 17*, 1707–1724.

Poblet, J., & McClay, K. (1996). Geometry and kinematics of single-layer detachment folds. *American Association of Petroleum Geologists Bulletin, 80*(7), 1085–1109.

Rafini, S., & Mercier, E. (2002). Forward modelling of foreland basins progressive unconformities. *Sedimentary Geology, 146*, 75–89.

Riba, O. (1976). Tectonogenèse et sédimentation: deux modèles de discordances syntectoniques pyrénéennes. *Bulletin du Bureau de Recherches Géologiques et Minières (BRGM) (2ème série), 1*(4), 383–401.

Riley, P., Gordon, C., Simo, J. A., Tikoff, B., & Soussi, M. (2011). Structure of the Alima and associated anticlines in the foreland basin of the southern Atlas Mountains, Tunisia. *Lithosphere, 3*(1), 76–91.

Rouchy, J. M. (1999). Un évènement exceptionnel: la crise de salinité messinienne de Méditerranée. In H.-J. Schubnel & F. Fröhlich (Eds.), *Les âges de la terre* (pp. 104–108). Paris: Muséum national d'histoire naturelle.

Salvini, F., & Storti, F. (2002). Three-dimensional architecture of growth-strata associated to fault-bend, fault-propagation, and decollement anticlines in non-erosional environments. *Sedimentary Geology, 146*, 57–73.

Salvini, F., Storti, F., & McClay, K. (2001). Self-determining numerical modeling of compressional fault-bend folding. *Geology, 29*, 839–842.

Shaw, J. H., & Suppe, J. (1994). Active faulting and growth folding in the eastern Santa Barbara Channel, California. *Geological Society of America Bulletin, 106*, 607–626.

Storti, F., & Poblet, J. (1997). Growth-stratal architectures associated to decollement folds and fault-propagation folds. Interferences on fold kinematics. *Tectonophysics, 282*, 353–373.

Suppe, J. (1983). Geometry and kinematics of fault-bend folding. *American Journal of Science, 283*, 684–721.

Suppe, J., Chou, G. T., & Hook, S. C. (1992). Rates of faulting determined from growth-strata. In K. R. McClay (Ed.), *Thrust tectonics* (pp. 105–121). London: Chapman and Hall.

Suppe, J., Sabat, F., Munoz, J. A., Poblet, J., Roca, E., & Vergès, J. (1997). Bed-by-bed fold growth by kink-band migration: Sant Llorenç de Morunys, eastern Pyrenees. *Journal of Structural Geology, 19*(34), 443–461.

Swezey, C. S. (1996). Structural controls on Quaternary depocenters within the Chotts trough region of southern Tunisia. *Journal of African Earth Sciences, 22*(3), 335–347.

Tavani, S., Storti, F., & Salvini, F. (2007). Modelling growth-stratal architectures associated with double edge fault-propagation folding. *Sedimentary Geology, 196*, 119–132.

Tricart, P., Torelli, L., Argnani, A., Rekhiss, F., & Zitellini, N. (1994). Extensional collapse related to compressional uplift in the alpine chain off northern Tunisia (Central Mediterranean). *Tectonophysics, 1–4*, 317–329.

Van Vliet-Lanoë, B. (2005). *La planète des glaces. Histoire et environnements de notre ère glaciaire*. Paris: Vuibert.

Weijermars, R. (1988). Neogene tectonics in the western Mediterranean may have caused the Messinian salinity crisis and an associated glacial event. *Tectonophysics, 148*, 211–219.

Wickham, J. (1995). Fault displacement-gradient folds and the structure at Lost Hills, California (USA). *Journal of Structural Geology, 17*(9), 1293–1302.

Zapata, T. R., & Allmendinger, R. W. (1996). Growth-stratal records of instantaneous and progressive limb rotation in the Precordillera thrust belt and Bermejo basin, Argentina. *Tectonics, 15*, 1065–1083.

Zargouni, F. (1984). Style et chronologie des deformations des structures de 1'Atlas tunisien meridional. Evolution recente de l'accident Sud-atlasique. *Comptes Rendus Academic Sciences (Paris), 299*, 71–76.

Zoetmeijer, R. (1993). *Tectonic modelling of foreland basins*. Amsterdam: University of Vrije.

Zouari, H. (1995). Evolution géodynamique de l'Atlas centro-méridional de la Tunisie: stratigraphie, analyses géométrique, cinématique et tectono-sédimentaire. Thèse de Doctorat d'Etat, Université de Tunis II.